Monthly Notices
of the
ROYAL ASTRONOMICAL SOCIETY

Mon. Not. R. Astron. Soc. **410,** 1631–1636 (2011) doi:10.1111/j.1365-2966.2010.17550.x

WASP-25b: a 0.6$M_{\rm J}$ planet in the Southern hemisphere

B. Enoch,[1⋆] A. Collier Cameron,[1] D. R. Anderson,[2] T. A. Lister,[3] C. Hellier,[2] P. F. L. Maxted,[2] D. Queloz,[4] B. Smalley,[2] A. H. M. J. Triaud,[4] R. G. West,[5] D. J. A. Brown,[1] M. Gillon,[4,6] L. Hebb,[7] M. Lendl,[4] N. Parley,[1] F. Pepe,[4] D. Pollacco,[8] D. Segransan,[4] E. Simpson,[8] R. A. Street[3] and S. Udry[4]

[1]*School of Physics and Astronomy, University of St Andrews, North Haugh, St Andrews KY16 9SS*
[2]*Astrophysics Group, Keele University, Staffordshire ST5 5BG*
[3]*Las Cumbres Observatory, 6740 Cortona Drive Suite 102, Goleta, CA 93117, USA*
[4]*Observatoire astronomique de l'Universitén de Genéve, 51 Chemin des Maillettes, 1290 Sauverny, Switzerland*
[5]*Department of Physics and Astronomy, University of Leicester, Leicester LE1 7RH*
[6]*Institut d'Astrophysique et de Géophysique, Université de Liége, Allée de 6 Août, 17, Bat B5C, Liége 1, Belgium*
[7]*Vanderbilt University, Department of Physics and Astronomy, Nashville, TN 37235, USA*
[8]*Astrophysics Research Centre, School of Mathematics & Physics, Queen's University, University Road, Belfast BT7 1NN*

Accepted 2010 August 16. Received 2010 July 22; in original form 2010 April 13

ABSTRACT

We report the detection of a 0.6 $M_{\rm J}$ extrasolar planet by WASP-South, WASP-25b, transiting its solar-type host star every 3.76 d. A simultaneous analysis of the WASP, FTS and Euler photometry and CORALIE spectroscopy yields a planet of $R_{\rm p} = 1.22 R_{\rm J}$ and $M_{\rm p} = 0.58 M_{\rm J}$ around a slightly metal-poor solar-type host star, [Fe/H] $= -0.05 \pm 0.10$, of $R_* = 0.92\,{\rm R}_\odot$ and $M_* = 1.00\,{\rm M}_\odot$. WASP-25b is found to have a density of $\rho_{\rm p} = 0.32\,\rho_{\rm J}$, a low value for a sub-Jupiter mass planet. We investigate the relationship of planetary radius to planetary equilibrium temperature and host star metallicity for transiting exoplanets with a similar mass to WASP-25b, finding that these two parameters explain the radii of most low-mass planets well.

Key words: planetary systems.

1 INTRODUCTION

To date, over 440 exoplanets have been discovered, including more than 70 detected by the transit method.[1] The transit method together with follow-up radial velocity observations allow measurement of both the mass and radius of the planet, leading to a value for the planet's bulk density (Charbonneau et al. 2000). The atmospheric composition of transiting exoplanets can also be investigated through high-precision photometric and spectroscopic measurements, see e.g. Charbonneau et al. (2002).

A wide range of transiting exoplanets radii has been found and there has been much investigation into the factors that may influence a planet's radius. For example, Guillot et al. (2006) propose a negative relationship between the metallicity of a host star and the radius of an orbiting planet, caused by an increase in the amount of heavy elements in the planet, leading to a more massive core and hence smaller radius for a given mass. Alternatively, Burrows et al. (2007) consider that increasing the metallicity may increase the opacity of an exoplanet's atmosphere, retarding cooling and leading to a larger radius for a given mass. Another influence on a planet's radius may be the equilibrium temperature of the planet (Guillot & Showman 2002), determined by the stellar irradiation and the planet's distance from its host star. Tidal heating due to the circularization of the orbits of close-in exoplanets may also play a role in inflating the planetary radius (Bodenheimer, Laughlin & Lin 2003; Jackson, Greenberg & Barnes 2008). One motivation of the SuperWASP project is to detect enough transiting exoplanets, with a wide range of orbital and compositional parameters, to allow analyses that may distinguish between such differing models.

In this paper, we report the discovery of a 0.6$M_{\rm J}$ planet orbiting a solar mass star, WASP-25 (TYC6706-861-1, 1SWASP J130126.36-273120.0), in the Southern hemisphere. Analysis of photometric and spectroscopic data reveals WASP-25b to be another low-density planet, comparable to HD 209458b (Charbonneau et al. 2000). We also analyse the dependence of the radii of low-mass planets on host star metallicity and planetary equilibrium temperature, including WASP-25b and 18 other transiting planets, finding a relationship using singular value decomposition (SVD) analysis that gives an excellent agreement between observed and calibrated radii.

In Section 2 we describe the photometric and spectroscopic observations and data reduction procedures. In Section 3 we present the stellar and planetary parameters extracted from these data. Finally,

⋆E-mail: becky.enoch@st-andrews.ac.uk
[1] www.exoplanet.eu

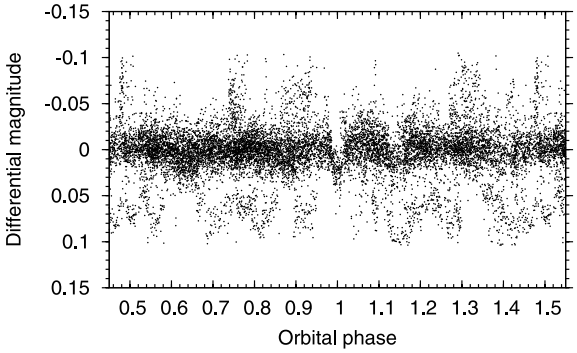

Figure 1. WASP discovery light curve folded on the orbital period of $P = 3.765$ d. Points with error above $3\times$ *median* were clipped, where *median* = 0.012 mag.

in Section 4 we compare WASP-25b with the ensemble of known planets of similar mass, and examine the relationship between stellar metallicity, irradiating flux (via the planet's equilibrium temperature) and planet radius.

2 OBSERVATIONS

2.1 Photometric observations

The WASP-South observatory is located at South African Astronomical Observatory (SAAO) in South Africa, and consists of eight 11-cm telescopes of 7.°8 × 7.°8 field of view each, on a single fork mount. The cameras scan repeatedly through 8–10 sets of fields, taking 30-s exposures. See Pollacco et al. (2006) for more details on the WASP project and the data reduction procedure, and Collier Cameron et al. (2007) and Pollacco et al. (2008) for an explanation of the candidate selection process.

WASP-25 was observed by WASP-South in 2006, 2007 and 2008, producing a total of 14 186 photometric data points. The 2007 data set showed the transit event most clearly, detected at a period of 3.76 d. Fig. 1 shows the WASP-South discovery light curve, using data from all seasons.

Further photometric observations were subsequently obtained on 2010 April 3 using the LCOGT 2-m Faulkes Telescope South (FTS) at Siding Spring, Australia. Observations were obtained using the fs01 Spectral camera containing a 4096 × 4096 pixel Fairchild CCD which was binned 2 × 2 giving 0.303 arcsec pixel^{-1} and a field of view of ∼10 × 10 arcmin^2. 285 data points were obtained through a Pan-STARRS z filter, capturing an entire transit.

The data were pre-processed through the WASP Pipeline (Pollacco et al. 2006) to perform masterbias/flat creation, debiasing and flat-field correction in the standard manner. Object detection and aperture photometry were performed using the DAOPHOT (Stetson 1987) package within the IRAF environment[2] with an aperture size of 18 binned pixels. Differential magnitudes of WASP-25 were formed by a weighted combination of the flux relative to 26 comparison stars within the field of view.

A second full transit was observed a week later on 2010 April 10 in the R band with EulerCam on the 1.2-m telescope at La Silla, Chile, comprising 204 data points. The resulting light curves are shown in Fig. 2.

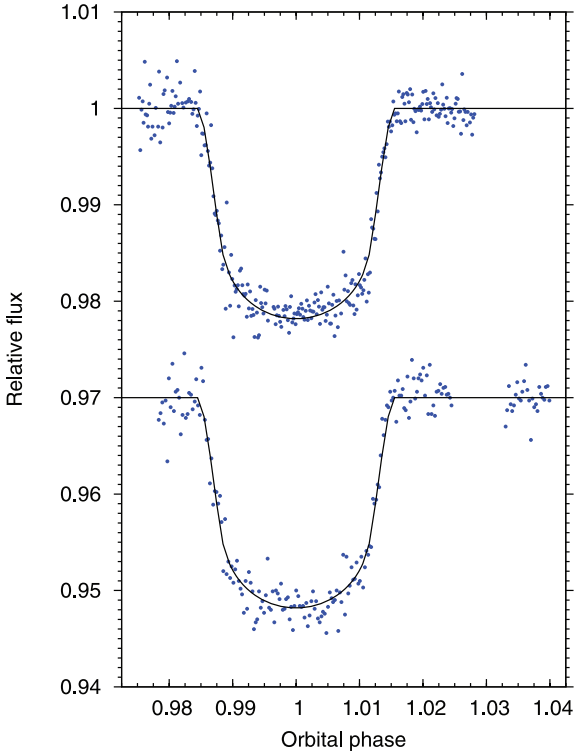

Figure 2. Top light curve: FTS follow-up photometry of WASP-25 on 2010 April 3. The central transit time is at HJD = 5290.056 17. Bottom light curve: Euler photometry on 2010 April 10 with central transit time at HJD = 5297.585 52.

2.2 Spectroscopic observations

WASP-25, a $V_{\rm mag} = 11.9$ star, was observed 29 times with the CORALIE spectrograph on the 1.2-m Euler telescope, between 2008 December 29 and 2009 June 28. The spectra were processed using the standard data reduction pipeline for CORALIE (Baranne et al. 1996; Mayor et al. 2009), plus a correction for the blaze function (Triaud et al. 2010). These data are given in Table 1 and shown phase-folded in Fig. 3: the low-amplitude radial velocity variations and the lack of correlation between the bisector spans and radial velocity (Queloz et al. 2001), shown in Fig. 4, are consistent with a planet-mass object orbiting the host star.

3 SYSTEM PARAMETERS

3.1 Stellar parameters

The CORALIE spectra were placed on a common wavelength scale and co-added to produce a higher signal-to-noise ratio spectrum, allowing an analysis of the host star and thus measurement of the stellar temperature, gravity, metallicity, $v \sin i$ and elemental abundances, given in Table 2, where η is microturbulence. The spectral data were analysed using the UCLSYN spectral synthesis package (Smalley, Smith & Dworetsky 2001) and ATLAS9 models without convective overshooting (Castelli, Gratton & Kurucz 1997). The effective temperature and $\log g$ were determined using the Hα and Hβ lines, and the Na I D and Mg I b lines, respectively, while the Ca H&K lines provided a check on those values. Further details of

[2] IRAF is distributed by the National Optical Astronomy Observatory, which is operated by the Association of Universities for Research in Astronomy (AURA) under cooperative agreement with the National Science Foundation.

Table 1. CORALIE radial velocity (RV) measurements of WASP-25.

BJD − 240 0000	RV (km s^{-1})	σ_{RV} (km s^{-1})	BS (km s^{-1})
54829.8227	−2.577	0.013	−0.019
54896.7698	−2.651	0.011	−0.022
54940.7092	−2.716	0.012	0.010
54941.7043	−2.619	0.012	−0.012
54942.7257	−2.576	0.012	−0.029
54943.6374	−2.618	0.012	−0.055
54944.7155	−2.680	0.012	−0.032
54945.7265	−2.615	0.013	−0.011
54946.6166	−2.582	0.013	−0.019
54947.6016	−2.641	0.011	−0.000
54947.7912	−2.689	0.013	0.001
54948.6130	−2.704	0.011	−0.011
54949.8031	−2.551	0.018	−0.030
54950.6221	−2.591	0.013	−0.044
54951.6953	−2.701	0.012	−0.011
54971.6453	−2.678	0.021	0.026
54972.6724	−2.561	0.013	0.027
54973.5157	−2.587	0.013	−0.030
54974.6787	−2.714	0.014	−0.064
54975.5379	−2.667	0.014	−0.023
54976.6837	−2.556	0.013	−0.011
54982.6194	−2.664	0.021	−0.029
54983.6213	−2.568	0.015	0.043
54983.6446	−2.597	0.015	−0.029
54984.5785	−2.558	0.015	0.023
54985.6100	−2.699	0.012	0.004
54995.5555	−2.509	0.014	−0.061
55009.6287	−2.606	0.018	0.018
55010.5967	−2.539	0.023	−0.036

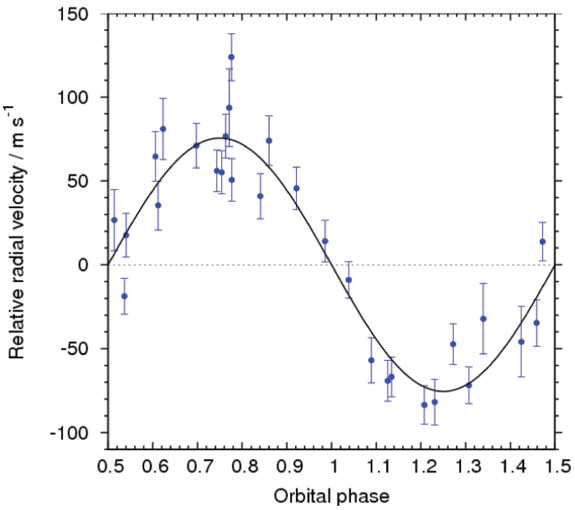

Figure 3. Radial velocity measurements. The solid line is the best-fitting MCMC solution. The centre-of-mass velocity, $\gamma = -2.6323$ km s^{-1}, was subtracted.

the spectral analysis are given in West et al. (2009a). The analysis yielded $T_{\rm eff} = 5750 \pm 100$ K and [Fe/H] $= -0.05 \pm 0.10$.

3.2 System parameters

The WASP-South, FTS and Euler photometry were simultaneously analysed with the CORALIE radial velocity data in a Markov chain

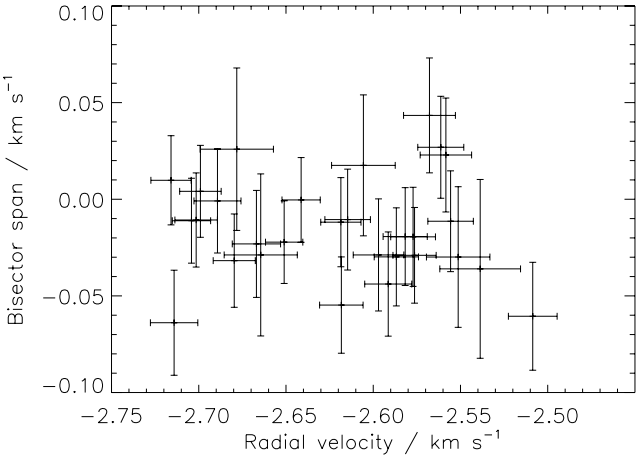

Figure 4. Bisector spans versus radial velocity, where bisector uncertainties are taken to be equal to twice the radial velocity uncertainties.

Table 2. Stellar parameters of WASP-25.

Parameter	Value
$T_{\rm eff}$	5750 ± 100 K
log g	4.5 ± 0.15
η	1.1 ± 0.1 km s^{-1}
v sin i	3.0 ± 1.0 km s^{-1}
Spectral type	G4
[Fe/H]	−0.05 ± 0.10
[Si/H]	0.00 ± 0.06
[Ca/H]	0.08 ± 0.14
[Ti/H]	0.04 ± 0.07
[Ni/H]	−0.08 ± 0.10
log[Li/H]	1.63 ± 0.09
V (mag)	11.88

1 SWASP J130126.36-273120.0

Monte Carlo (MCMC) analysis. This analysis is described in Collier Cameron et al. (2007), but is here modified as described in Enoch et al. (2010) to determine stellar mass using a calibration on $T_{\rm eff}$, log ρ and [Fe/H] [similar to the $T_{\rm eff}$, log g and [Fe/H] calibration described in Torres, Andersen & Giménez (2009)]. The temperature and metallicity were obtained through spectral analysis (given in Table 2), and the density is determined directly from the photometry. Mass and radius values obtained for other WASP host stars via this method agree closely with values obtained through isochrone analysis.

An initial analysis was performed allowing the eccentricity value to float, producing a value of $e = 0.123^{+0.041}_{-0.046}$. This eccentricity value is consistent with 0 at the 3σ level, and was suspected to not be significant, as can occur from spurious asymmetries in quadrature fits due to noise (Laughlin et al. 2005), so a second analysis was performed with eccentricity fixed to 0. We performed an F-test on the radial velocity residuals from the circular and floating eccentricity fits, resulting in a value of 0.897 which shows that the eccentric fit is not significant.

The resulting circular model best-fitting parameters for the star–planet system are listed in Table 3, using the best-fitting parameters from the $e = 0$ fit and the uncertainties from the fit allowing eccentricity to float, to sufficiently account for uncertainty due to unknown eccentricity. The results show WASP-25 to be a solar analogue of

Table 3. System parameters of WASP-25.

Parameter	Symbol	Value
Period (d)	P	$3.764\,825 \pm 0.000\,005$
Transit epoch (HJD)	T_0	$5274.996\,49 \pm 0.000\,17$
Transit duration (d)	D	0.116 ± 0.001
Planet/star area ratio	R_p^2/R_*^2	0.0187 ± 0.0002
Impact parameter	b	$0.38^{+0.06}_{-0.07}$
Stellar reflex velocity ($m\,s^{-1}$)	K_1	75.5 ± 5.3
Centre-of-mass velocity ($m\,s^{-1}$)	γ	-2632.3 ± 0.6
Orbital separation (au)	a	0.0473 ± 0.0004
Orbital inclination (°)	i	88.0 ± 0.5
Orbital eccentricity	e	0 (adopted)
Stellar mass ($M_\odot$)	M_*	1.00 ± 0.03
Stellar radius ($R_\odot$)	R_*	0.92 ± 0.04
Stellar surface gravity ($\log g_\odot$)	$\log g_*$	4.51 ± 0.03
Stellar density ($\rho_\odot$)	ρ_*	1.29 ± 0.10
Stellar metallicity	[Fe/H]	-0.07 ± 0.10
Stellar effective temperature	$T_{\rm eff}$	5703 ± 100
Planet mass (M_J)	M_p	0.58 ± 0.04
Planet radius (R_J)	R_p	$1.22^{+0.06}_{-0.05}$
Planet surface gravity ($\log g_J$)	$\log g_p$	2.95 ± 0.04
Planet density (ρ_J)	ρ_p	$0.317^{+0.036}_{-0.031}$
Planet temperature ($A = 0, F = 1$) (K)	$T_{\rm eq}$	1212 ± 35

one solar mass and 0.92 ± 0.04 solar radius, and WASP-25b to be a bloated hot Jupiter of $0.58 \pm 0.04 M_J$ and $1.22 \pm 0.06 R_J$, giving a planet density of $\rho = 0.32^{+0.04}_{-0.03}\,\rho_J$.

The stellar density of $1.29 \pm -0.11\,\rho_\odot$ obtained from the MCMC analysis was used along with the determined stellar temperature and metallicity values in an interpolation of the Girardi et al. (2000) stellar evolution tracks, see Fig. 5. Using the best-fitting metallicity of -0.07 indicates that WASP-25 has a mass of $1.02^{+0.03}_{-0.07}\,M_\odot$, agreeing well with the calibrated MCMC result of $1.00 \pm 0.03\,M_\odot$ and an age of $0.02^{+3.96}_{-0.01}$ Gyr.

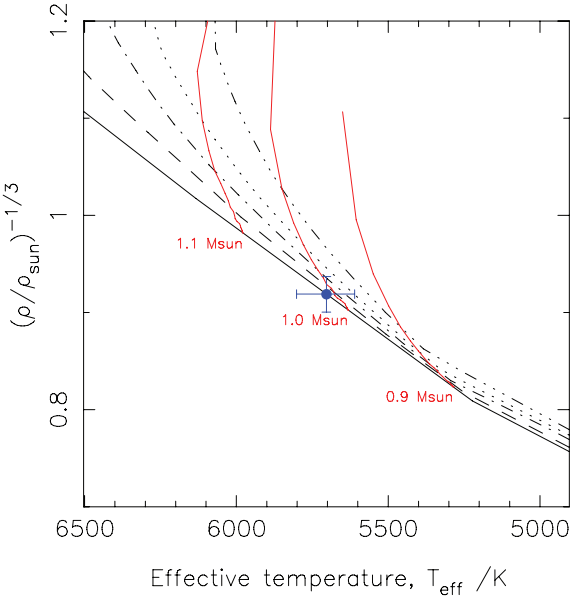

Figure 5. Isochrone tracks from Girardi et al. (2000) for WASP-25 using the best-fitting metallicity of -0.07 and stellar density $1.29\,\rho_\odot$. Isochrones are 0.019 95 Gyr (solid), 0.7943 Gyr (dashed), 1.99 Gyr (dot–dashed), 3.16 Gyr (dotted) and 5.01 Gyr (triple dot–dashed).

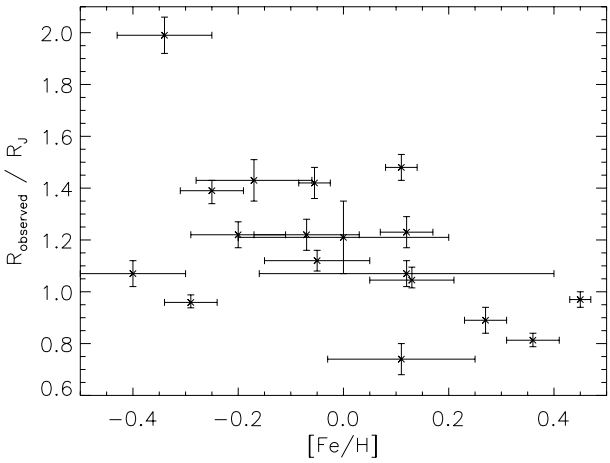

Figure 6. Radius versus metallicity of 18 planets of 0.1–0.6M_J.

4 DISCUSSION

A density of $0.32^{+0.04}_{-0.03}\,\rho_J$ places WASP-25b amongst the bloated hot Jupiters, with over 80 per cent of known transiting exoplanets being more dense.[3] Guillot et al. (2006) proposed a correlation between the metallicity of a host star and the amount of heavy elements present in the planet. A larger amount of heavy elements is likely to produce a more massive rocky core and hence would lead to larger planetary radii for lower metallicity stars, for a given planetary mass (Fressin et al. 2007). Alternatively, the heavy elements could increase the opacity of the planetary interior, potentially increasing the radius (Burrows et al. 2007).

WASP-25b has a mass close to the value above which the gravitational, potential energy begins to exceed the electrical binding energy of electrons in atoms as the main force opposing electron degeneracy pressure in the deep planetary interior (Lynden-Bell & O'Dwyer 2001). It is in this lower mass range that we see the greatest range of radii at a given mass. This suggests that environmental and compositional differences between individual planets have the greatest influence on their radii in this mass range.

To investigate this relationship, we calculated the correlation between radius and metallicity for all known transiting exoplanets for which metallicity data were available (67 planets), finding only a very weak relationship with a correlation coefficient of -0.17. However, splitting the planets into low-mass (0.1–0.6M_J) and higher mass ($>0.6M_J$) sets resulted in correlation coefficients of -0.53 (with a probability of no correlation of 0.022) and 0.07, respectively, indicating that metallicity plays a role in determining the radii of low-mass planets but not those of higher mass. We plot the radii against host star metallicity of low-mass planets in Fig. 6. We concentrate on the set of 18 low-mass planets, of which nine are WASP planets, including WASP-25b, see Table 4), in further investigating planetary radii.

A major influence on the radius of an exoplanet is likely to be the planet's equilibrium temperature (Fressin et al. 2007), $T_{\rm eq}$, defined as

$$T_{\rm eq} = T_{*,\rm eff}\left(\frac{1-A}{F}\right)\sqrt{\frac{R_*}{2a}}, \quad (1)$$

where $T_{*,\rm eff}$ is the host star's effective temperature, R_* is the stellar radius, a is the semimajor axis, A is the planetary Bond albedo and

[3] www.exoplanet.eu

Table 4. Details of the 18 low-mass planets.

Planet	M_p/M_J	R_p/R_J	a (au)	$T_{*,eff}$ (K)	[Fe/H]	$R_*/R_\odot$	T_{eq} (K)	Reference
HAT-12b	0.21	$0.96^{+0.03}_{-0.02}$	0.0384 ± 0.0003	4650 ± 60	-0.20 ± 0.05	$0.70^{+0.02}_{-0.01}$	957^{+30}_{-23}	Hartman et al. (2009)
WASP-29b	0.25	0.74 ± 0.06	0.0456 ± 0.0006	4800 ± 150	0.11 ± 0.14	0.85 ± 0.05	997^{+67}_{-65}	Hellier et al. (2010)
WASP-21b	0.30	1.07 ± 0.05	0.0520 ± 0.0004	5800 ± 100	-0.4 ± 0.1	$1.01^{+0.02}_{-0.03}$	1263^{+51}_{50}	Bouchy et al. (2010)
HD149026b	0.37	0.81 ± 0.03	$0.0431^{+0.0007}_{-0.0006}$	6147 ± 50	0.36 ± 0.05	$1.54^{+0.05}_{-0.04}$	1772^{+53}_{-52}	Sato et al. (2005), Carter et al. (2009)
Kepler-7b	0.43	$1.48^{+0.05}_{-0.05}$	$0.0622^{+0.0011}_{-0.0008}$	5933 ± 44	0.11 ± 0.03	$1.84^{+0.07}_{-0.07}$	1556^{+52}_{-54}	Latham et al. (2010)
WASP-11b	0.46	$1.045^{+0.05}_{-0.03}$	$0.043^{+0.002}_{-0.002}$	4980 ± 60	0.13 ± 0.08	$0.81^{+0.03}_{0.03}$	1042^{+58}_{-55}	West et al. (2009b)
WASP-13b	0.46	$1.21^{+0.14}_{-0.14}$	$0.0527^{+0.0017}_{-0.0019}$	5826 ± 100	0.0 ± 0.2	$1.34^{+0.13}_{-0.13}$	1416^{+121}_{-114}	Skillen et al. (2009)
CoRoT-5b	0.47	$1.39^{+0.04}_{-0.05}$	$0.0495^{+0.0003}_{-0.0003}$	6100 ± 65	-0.25 ± 0.06	$1.19^{+0.04}_{-0.04}$	1442^{+44}_{-43}	Rauer et al. (2009)
WASP-17b	0.49	1.99 ± 0.07	$0.0518^{+0.0017}_{-0.0018}$	6600 ± 100	-0.34 ± 0.09	$1.38^{+0.19}_{-0.19}$	1645^{+169}_{-166}	Anderson et al. (2010)
WASP-6b	0.50	$1.22^{+0.05}_{-0.05}$	$0.0421^{+0.0008}_{-0.0013}$	5450 ± 100	-0.20 ± 0.09	$0.87^{+0.03}_{-0.04}$	1195^{+59}_{-57}	Gillon et al. (2009)
HAT-1b	0.52	$1.23^{+0.06}_{-0.06}$	$0.0553^{+0.0014}_{-0.0014}$	6047 ± 56	0.12 ± 0.05	$1.12^{+0.05}_{-0.05}$	1309^{+59}_{-57}	Bakos et al. (2007)
OGLE-111b	0.53	$1.07^{+0.05}_{-0.05}$	$0.047^{+0.001}_{-0.001}$	5070 ± 400	0.12 ± 0.28	$0.83^{+0.03}_{-0.03}$	1028^{+114}_{-109}	Pont et al. (2004)
WASP-15b	0.54	$1.43^{+0.08}_{-0.08}$	$0.0499^{+0.0018}_{-0.0018}$	6300 ± 100	-0.17 ± 0.11	$1.48^{+0.07}_{-0.07}$	1653^{+99}_{-94}	West et al. (2009a)
WASP-22b	0.56	$1.12^{+0.04}_{-0.04}$	$0.0468^{+0.0004}_{-0.0004}$	6000 ± 100	-0.05 ± 0.1	$1.13^{+0.03}_{-0.03}$	1421^{+49}_{-48}	Maxted et al. (2010)
XO-2b	0.57	$0.97^{+0.03}_{-0.03}$	$0.037^{+0.002}_{-0.002}$	5340 ± 32	0.45 ± 0.02	$0.96^{+0.02}_{-0.02}$	1315^{+59}_{-55}	McCullough et al. (2006)
WASP-25b	0.58	$1.26^{+0.06}_{-0.06}$	$0.0474^{+0.0004}_{-0.0004}$	5750 ± 100	-0.05 ± 0.02	$0.95^{+0.04}_{-0.04}$	1241^{+55}_{-55}	–
HAT-3b	0.60	$0.89^{+0.05}_{-0.05}$	$0.0389^{+0.0007}_{-0.0007}$	5185 ± 46	0.27 ± 0.04	$0.82^{+0.04}_{-0.04}$	1150^{+51}_{-45}	Torres et al. (2007)
Kepler-8b	0.60	$1.42^{+0.06}_{-0.06}$	$0.0483^{+0.0006}_{-0.0012}$	6213 ± 150	-0.055 ± 0.03	$1.49^{+0.06}_{-0.06}$	1662^{+98}_{-84}	Jenkins et al. (2010)

F is the fraction of the planet reradiating flux. Jupiter has a Bond albedo of 0.28 (Taylor 1965) but albedo values have not so far been determined for the majority of exoplanets, and Rowe et al. (2008) found a very low albedo for HD 209458b, at just 0.04 ± 0.05. We set $A = 0$ ($F = 1$) here to calculate the equilibrium temperatures. Not knowing the true albedo values for all the planets studied here produces an uncertainty in the values calculated for equilibrium temperature of $(1 - A)^{1/4}$. We find the correlation coefficient between the (approximate) equilibrium temperature and radius of all 18 planets to be 0.55, a moderate relationship, shown in Fig. 7. The correlation of radii and equilibrium temperature is stronger than this for the majority of planets – removing the two outliers, WASP-17b and HD 149026b, from the correlation produces a coefficient of 0.82 for the remaining 16 planets, a strong relationship. Accurate albedo values, and hence equilibrium temperatures, may produce an even stronger correlation than found here.

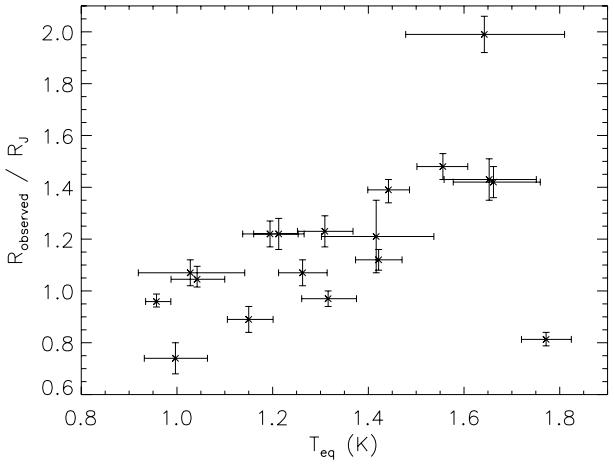

Figure 7. Radius versus equilibrium temperature of 18 planets of 0.1–0.6M_J.

Since both the host star metallicity and the planet's equilibrium temperature seem to explain the radii of low-mass planets in part, we performed a weighted SVD fit to fully quantify the relationship. This resulted in the equation

$$R_p = 0.48 + 0.50(T_{eq}/1000\,\mathrm{K}) - 0.61[\mathrm{Fe/H}], \quad (2)$$

producing the fit to the planetary radii shown in Fig. 8. Removing the two outliers mentioned above, WASP-17b and HD 149026b, leads to a much better fit, shown in Fig. 9, implying that additional parameters particularly affect these two planets. The SVD fit for the 16 planets is

$$R_p = 0.20 + 0.73(T_{eq}/1000\,\mathrm{K}) - 0.25[\mathrm{Fe/H}]. \quad (3)$$

The negative slope of the metallicity correlation and of the SVD coefficient implies that the effect of a massive core (Guillot et al. 2006) outweighs the effect of increased opacity in the interior of the planet, i.e. increased metallicity leads to a smaller planetary radius.

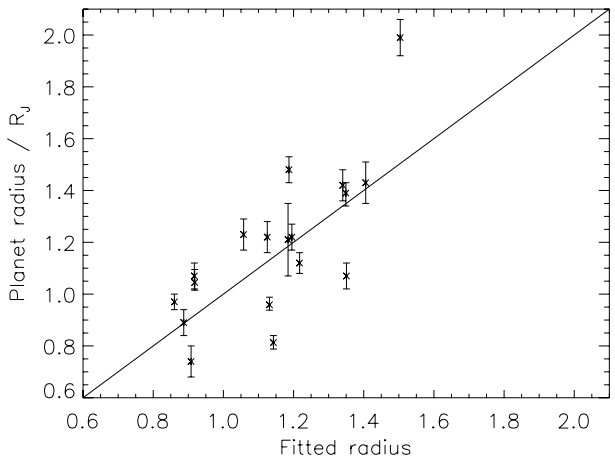

Figure 8. Results of SVD fit on the radii of 18 planets of 0.1–0.6M_J.

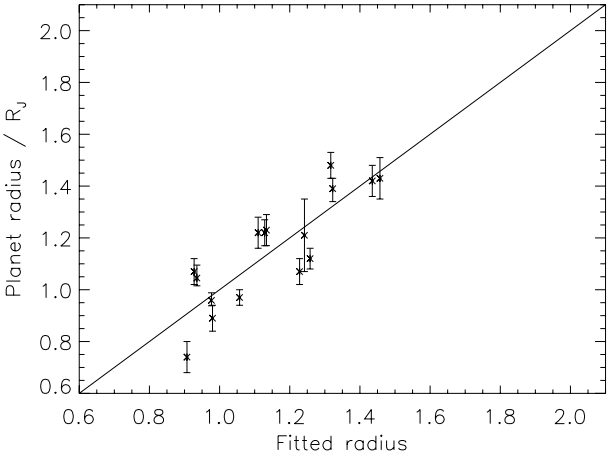

Figure 9. Results of SVD fit on the radii of planets of 0.1–0.6M_J, excluding WASP-17b and HD 149026b.

5 CONCLUSIONS

We have reported the detection of a 0.58M_J planet, WASP-25b, transiting a slightly metal-poor solar-mass star in the Southern hemisphere with an orbital period of 3.76 d. WASP-25b has a low density, 0.29 ρ_J, and we investigate its bloated radius, $R_p = 1.26\,R_J$. We find that the radii of most transiting exoplanets of a similar mass to WASP-25b can be explained well by a calibration to the host star metallicity and planetary equilibrium temperature.

ACKNOWLEDGMENTS

WASP-South is hosted by the South African Astronomical Observatory and we are grateful for their ongoing support and assistance. Funding for the WASP comes from consortium universities and from the UK's Science and Technology Facilities Council.

REFERENCES

Anderson D. R. et al., 2010, ApJ, 709, 159
Bakos G. Á. et al., 2007, ApJ, 656, 552
Baranne A. et al., 1996, A&AS, 119, 373
Bodenheimer P., Laughlin G., Lin D. N. C., 2003, ApJ, 592, 555
Bouchy F. et al., 2010, A&A, 519, 98
Burrows A., Hubeny I., Budaj J., Hubbard W. B., 2007, ApJ, 661, 502
Carter J. A., Winn J. N., Gilliland R., Holman M. J., 2009, ApJ, 696, 241
Castelli F., Gratton R. G., Kurucz R. L., 1997, A&A, 318, 841
Charbonneau D., Brown T. M., Latham D. W., Mayor M., 2000, ApJ, 529, L45
Charbonneau D., Brown T. M., Noyes R. W., Gilliland R. L., 2002, ApJ, 568, 377
Collier Cameron A. et al., 2007, MNRAS, 380, 1230
Enoch B., Cameron A. C., Parley N. R., Hebb L. H., 2010, A&A, 516, 33
Fressin F., Guillot T., Morello V., Pont F., 2007, A&A, 475, 729
Gillon M., Anderson D. R., Triaud A. H. M. J., Hellier C., Maxted P. F. L., Pollaco D., Queloz D., 2009, A&A, 501, 785
Girardi L., Bressan A., Bertelli G., Chiosi C., 2000, VizieR Online Data Catalog, 414, 10371
Guillot T., Showman A. P., 2002, A&A, 385, 156
Guillot T., Santos N. C., Pont F., Iro N., Melo C., Ribas I., 2006, A&A, 453, L21
Hartman J. D. et al., 2009, ApJ, 706, 785
Hellier C. et al., 2010, submitted
Jackson B., Greenberg R., Barnes R., 2008, ApJ, 681, 1631
Jenkins J. M. et al., 2010, preprint (arXiv:1001.0486)
Latham D. W. et al., 2010, ApJ, 713, L140
Laughlin G., Marcy G. W., Vogt S. S., Fischer D. A., Butler R. P., 2005, ApJ, 629, L121
Lynden-Bell D., O'Dwyer J. P., 2001, preprint (astro-ph/0104450)
McCullough P. R. et al., 2006, ApJ, 648, 1228
Maxted P. F. L. et al., 2010, preprint (arXiv:1004.1514)
Mayor M. et al., 2009, A&A, 493, 639
Pollacco D. L. et al., 2006, PASP, 118, 1407
Pollacco D. et al., 2008, MNRAS, 385, 1576
Pont F., Bouchy F., Queloz D., Santos N. C., Melo C., Mayor M., Udry S., 2004, A&A, 426, L15
Queloz D. et al., 2001, A&A, 379, 279
Rauer H. et al., 2009, A&A, 506, 281
Rowe J. F. et al., 2008, ApJ, 689, 1345
Sato B. et al., 2005, ApJ, 633, 465
Skillen I. et al., 2009, A&A, 502, 391
Smalley B., Smith K., Dworetsky M., 2001, http://www.astro.keele.ac.uk/bs/publs/uclsyn.pdf
Stetson P. B., 1987, PASP, 99, 191
Taylor D. J., 1965, Icarus, 4, 362
Torres G. et al., 2007, ApJ, 666, L121
Torres G., Andersen J., Giménez A., 2010, A&AR, 18, 67
Triaud A. et al., 2010, preprint (arXiv:1008.2353)
West R. G. et al., 2009a, AJ, 137, 4834
West R. G. et al., 2009b, A&A, 502, 395

This paper has been typeset from a TEX/LATEX file prepared by the author.